

Total fusion excitation function using various potentials

H M M Mansour and Jannette W Guirguis

Department of Physics, Faculty of Science, Cairo University, Giza, Egypt

and

G S Hassan

Department of Physics, Faculty of Science, Assiut University, Egypt

Received 5 June 1992, accepted 4 February 1993

Abstract : Fusion reaction for various nuclear systems are analyzed using the double folding model with a factorized density and energy dependent interaction (FDDM3Y). The total fusion cross sections are calculated for different pairs of nuclei using either the sharp cut-off or smooth cut-off approximation. The results are compared with two commonly known potentials. Specifically we have chosen the proximity and the Woods-Saxon potential forms. The calculation based on FDDM3Y potential gives better agreement with the experimental data than the other common methods based on the proximity and the Woods-Saxon potentials. We used the Glas-Mosel model to fit the experimental data at high energies for the reactions $^{16}_8\text{O} + ^{27}_{13}\text{Al}$ and $^{16}_8\text{O} + ^{28}_{14}\text{Si}$.

Keywords : Fusion, nucleon-nucleon interaction, potential, density, energy.

PACS Nos. : 25.70.Jj, 21.30.+y

1. Introduction

Heavy ion fusion reaction have been studied and various theoretical methods have been introduced to interpret the observed data, yet a clear understanding is far from being established.

In a previous work [1], we used an effective nucleon-nucleon interaction (M3Y) to calculate the real part of potential between different pairs of spherical nuclei in the framework of double folding model. The results were compared with the experimental data and it was found that the agreement between the two occurs for $(A_1^{1/3} + A_2^{1/3}) < 7$. In spite of the success of the double folding model with M3Y-force to predict the interaction potential between two ions, evidence of the failure of the double folding model with M3Y-force has been found [2]. For these reasons different attempts have been made to improve this force. Recent modifications of M3Y force have been to include energy and density dependences [3,4].

The aim of present work is to check the validity of such modified potential by comparing with the experimental data for the fusion excitation function of several pairs of

nuclei at several bombarding energies. The fusion cross section is calculated using either the sharp cut-off or smooth cut-off approximations. Two other kinds of potentials (the proximity and the Woods-Saxon potentials) are examined and used to compare with the results obtained for the factorized density dependent potential (FDDM3Y).

In the next section, the analysis of low energy region as well as the high energy region are described. The forms of the different potentials are also given. The last section is devoted to the discussion of the results obtained.

2. Theory

The interaction potential between two nuclei separated by a relative distance R is defined as [5] :

$$V(R) = \frac{2}{\pi} \int_0^\infty dK J_0(KR) V_{12}(K) A_{00}^{(1)}(K) A_{00}^{(2)}(K) \quad (1)$$

where V_{12} is the two nucleon interaction and $A_{00}^{(i)}$ is defined as :

$$A_{00}^{(i)} = \int d\mathbf{r}_i r_i^2 \rho_i(r_i) J_0(Kr_i) \quad i = 1, 2$$

where $\rho_i(r_i)$ is the nuclear matter distribution of nuclei. For convenience, we have used the Fermi type distribution for the densities :

$$\rho(r) = \rho_0 / [1 + e^{(r-R_0)/a}] \quad (2)$$

The parameters ρ_0 , R_0 and a are taken from Ref. [3] or by using the method suggested in Ref. [6]. The Coulomb term $V_C(R)$ is obtained from eq. (1) by substituting $V_{12}(K) = 4/K^2$. The nuclear term is also obtained from eq. (1) by putting the Fourier transform of the (FDDM3Y) two nucleon interaction in the form [4] :

$$V_{12}(K) = C [1 - \beta \rho_1^{2/3}(r_1)][1 - \beta \rho_2^{2/3}(r_2)] \cdot [7999((4\pi)/4(K^2 + 16)) - 2134((4\pi)/2.5(K^2 + 6.25)) + J_\infty(E) \delta(r)] \quad (3)$$

with $J_\infty(E) = -276(1 - 0.005 E/A_p)$; $C = 1.3$, $\beta = 1.01$

The total real potential is given by :

$$V_T = V_C(R) + V_N(R). \quad (4)$$

The fusion cross section is given by

$$\sigma_F = \frac{\pi}{K^2} \sum_{l=0}^{\infty} (2l+1) T_l P_l \quad (5)$$

where T_l , P_l and K are the transmission, the fusion probability and the wavenumber, respectively.

In the sharp cut-off approximation, the fusion probability P_l is equal to one and the transmission probability is

$$T_l(E) = \begin{cases} 1 & \text{for } l \leq l_F \\ 0 & \text{for } l \geq l_F \end{cases}$$

The cross section in this case reads

$$\sigma_F = \pi R_{F,0}^2 \left[1 - \frac{V_{F,0}(R_F)}{E_{c.m.}} \right] \quad (6)$$

where $V_{F,0}$ is the total potential given by eq. (4) at a fusion radius $R_{F,0}$ and center of mass energy, $E_{c.m.}$.

This form has been commonly used for the heavy-ion reactions. However, eq. (5) is usually applied using the assumption that the barrier position independent of incident energy. Such energy dependence can be taken properly into account by using the following equations :

$$\begin{aligned} [V_c(r) + V_N(r) + V_l(r)]_{r=R} &= E \\ \frac{\partial}{\partial r} [V_c(r) + V_N(r) + V_l(r)]_{r=R} &= 0 \\ \frac{\partial^2}{\partial r^2} [V_c(r) + V_N(r) + V_l(r)]_{r=R} &< 0 \end{aligned} \quad (7)$$

where the centrifugal potential is denoted by $V_l(r)$ and the energy dependent position is denoted by R distinguished from the fixed $R_{F,0}$.

For the smooth cut-off approximation, the transmission coefficient is given by Hill-Wheeler equation

$$T_l(E) = 1/[1 + \exp \{2\pi (V_{F,l} - E_{c.m.})/\hbar\omega_l\}] \quad (8)$$

where $\omega_l = \{ \frac{1}{\mu} (\frac{\partial^2 V}{\partial R^2}) \}_{R=R_F}^{1/2}$ and $(\frac{\partial^2 V}{\partial R^2})_{R=R_F}$ is the stiffness coefficient at $R = R_F$.

In the present investigation, the calculation are performed using eqs. (5), (8) and (7) with $P_l = 1$.

Next, we introduce the Glas-Mosel formula [7] given by

$$\sigma_F = \left(\frac{\hbar\omega R_F^2}{2E} \right) \ln [1 + \exp \{ \frac{2\pi}{\hbar\omega} (E - V(R_F)) \}]. \quad (9)$$

This formula will be used for the cases where there is a need to limit the partial waves.

In the other Glas-Mosel mode [8] one usually simplifies eq. (9) into two conditions

(i) At low energies

$$\sigma_F = \pi R_B^2 \left[1 - \frac{V_B(R_B)}{E_{c.m.}} \right] \quad (10)$$

$$\text{with } R_B = 1.4 (A_p^{1/3} + A_T^{1/3}).$$

(ii) At high energies

$$\sigma_F = \pi R_{Cr}^2 \left[1 - \frac{V_{Cr}(R_{Cr})}{E_{c.m.}} \right] \quad (11)$$

$$\text{with } R_{Cr} = r_{Cr} (A_p^{1/3} + A_T^{1/3}) \text{ and } r_{Cr} = 1.0 \pm 0.07 \text{ fm.}$$

Two other simple forms of potentials used for comparison with the predictions of FDDM3Y calculation, *i.e.*

(i) *Woods-Saxon potential* :

The standard form of potential

$$V(r) = - \frac{V_0}{1 + \exp(r - R)/a}$$

where R , a and V_0 are parameters which are given for different reactions system by $V_0 = -10$ MeV, $R = 1.39 A^{1/3}$ fm and $a = 0.3$ fm except for the reaction $^{30}\text{Si} + ^{170}\text{Er}$, $V_0 = -16$ MeV.

(ii) *The proximity potential* :

The proximity potential [9] is based on the liquid drop model for the geometrical consideration and using the surface interaction, then nucleus-nucleus potential is universally written in terms of S , the distance between the planes of half-maximum density

$$V_N(S) = - \frac{da_s}{R_{12}} A_1^{1/3} A_2^{1/3} \exp(-S/d)$$

where the parameters : $d = 1.35$ fm, $a_s = 17$ MeV and $R_{12} = R_1 + R_2$ with $R_i = r_o A_i^{1/3}$ ($i = 1, 2$) and $r_o = 1.07$ fm.

3. Results and discussion

In the present work, 35 fusion reactions have been analyzed using the folding model eq. (1) with FDDM3Y force eq. (3). Table 1 gives the values of R_F obtained in the present calculations which gives a good fit with the available experimental cross sections some of these values are compared with previous works [10-12].

Figures 1 to 6 present the theoretical fusion cross sections which are calculated using the sharp cut-off approximation eq. (6) and the nuclear part of the real potential is calculated using the folding model eq. (1) with FDDM3Y force. Also on the same figures we present the calculation of the cross section using the nuclear part the other common form of Woods-Saxon and the proximity potentials. From these figures it is clear that the calculation using FDDM3Y potential yields an adequate fit with the experimental data [13, 14] in comparison with the other potentials. For some other data we used in calculating the fusion cross section the smooth cut-off approximation given by eq. (9) and the nuclear part of the real potential is evaluated using the FDDM3Y-force. Figure 7 shows a comparison

between this approximation and sharp cut-off one for the fusion reaction $^{64}\text{Ni} + ^{64}\text{Ni}$ using FDDM3Y and also using sharp cut-off approximation using for the nuclear part the other common form of potentials (Woods-Saxon and proximity potentials). From Figure 7 we

Table 1. Comparison between some of the values used for R_F in our work and the experimental values.

System	R_F (present work)	Experimental values of R_F Ref. [10]	R_F others Refs. [11,12]
$^{30}\text{Si} + ^{170}\text{Er}$	11.41		
$^{20}\text{Ne} + ^{133}\text{Cs}$	10.78		
$^{16}\text{O} + ^{148}\text{Sm}$	10.51	11.02	
$^{19}\text{F} + ^{181}\text{Ta}$	11.07		
$^{40}\text{Ar} + ^{165}\text{Ho}$	11.53	11.48	
$^{35}\text{Cl} + ^{141}\text{Pr}$	11.03	11.06	
$^{16}\text{O} + ^{181}\text{Ta}$	11.22		
$^{16}\text{O} + ^{150}\text{Sm}$	11.54	11.08	
$^{16}\text{O} + ^{208}\text{Pb}$	11.19, 11.48	11.74	
$^{35}\text{Cl} + ^{116}\text{Sn}$	10.69	10.81	
$^{20}\text{Ne} + ^{40}\text{Ca}$	8.69	9.36	
$^{40}\text{Ca} + ^{62}\text{Ni}$	10.16	10.35	
$^{35}\text{Cl} + ^{62}\text{Ni}$	9.79	10.29	9.5 ± 0.4 , 9.79
$^{12}\text{C} + ^{209}\text{Bi}$	11.42		
$^{12}\text{C} + ^{19}\text{F}$	7.75, 8.06	8.35	7.6 ± 0.2 , 7.75
$^{12}\text{C} + ^{24}\text{Mg}$	7.8		
$^{24}\text{Mg} + ^{24}\text{Mg}$	8.5		
$^{28}\text{Si} + ^{29}\text{Si}$	8.75		
$^{28}\text{Si} + ^{30}\text{Si}$	9.145		
$^{173}\text{Lu} + ^{12}\text{C}$	11.086		
$^{165}\text{Ho} + ^{14}\text{N}$	11.02		
$^{182}\text{W} + ^{12}\text{C}$	10.74		
$^{12}\text{C} + ^9\text{Be}$	7.48	7.65	
$^{18}\text{O} + ^{27}\text{Al}$	8.746	8.86	8.29 ± 0.3 , 8.37
$^{18}\text{O} + ^{28}\text{Si}$	8.37	8.76	
$^{16}\text{O} + ^{40}\text{Ca}$	8.97	9.21	9.00 ± 0.4 , 8.53
$^{24}\text{Mg} + ^{26}\text{Mg}$	8.5		
$^{64}\text{Ni} + ^{64}\text{Ni}$	10.73		
$^{40}\text{Ca} + ^{40}\text{Ca}$	9.31		
$^{32}\text{S} + ^{208}\text{Pb}$	11.68		
$^{58}\text{Fe} + ^{208}\text{Pb}$	12.09		
$^{32}\text{S} + ^{154}\text{Sm}$	11.23		
$^{40}\text{Ca} + ^{60}\text{Ni}$	9.9		
$^{16}\text{O} + ^{28}\text{Si}$	8.6	8.7	
$^{40}\text{Ca} + ^{58}\text{Ni}$	10.2	10.2	

can deduce that the smooth cut-off is better than the sharp cut-off, especially at high energy. Figures 8 and 9 show that for reactions like $^{16}\text{O} + ^{27}\text{Al}$ and $^{16}\text{O} + ^{28}\text{Si}$ the best fit

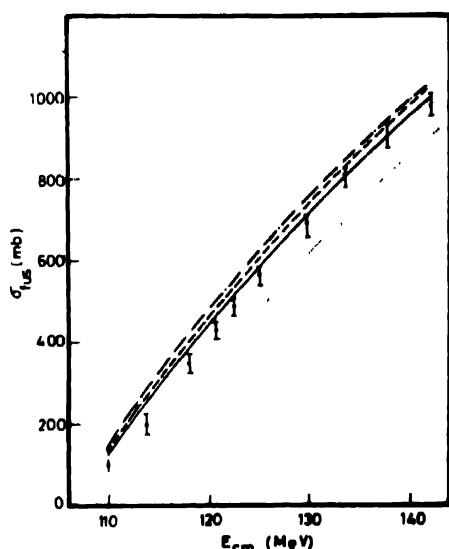


Figure 1. (Dashed line) represents the calculation of the excitation function for $^{30}\text{Si} + ^{170}\text{Er}$ reaction with sharp cut-off, M3Y-force and with $R_F = 11.3$ fm. (Full line) represents the same calculation as dashed line but with FDDM3Y-force and with $R_F = 11.4$ fm. (Dotted line) represents the same calculation with $R_F = 11.4$ fm and with Woods-Saxon potential as a nuclear part. (Dot-dashed line) represents the same as the dotted line but with proximity potential as a nuclear part. The experimental points are taken from Ref. (13).

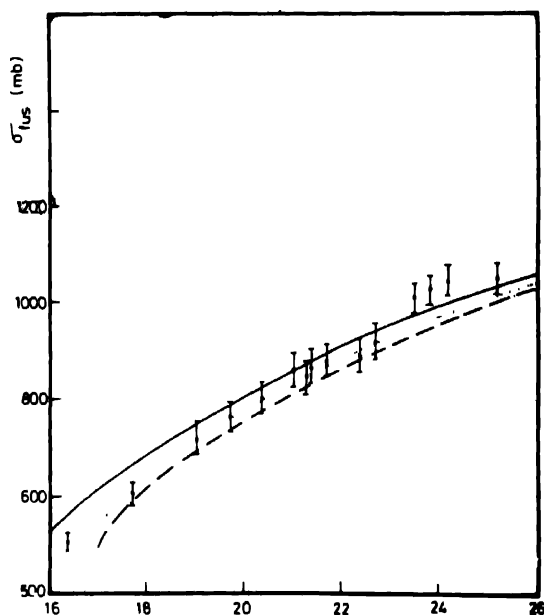


Figure 2. The same as Figure 1 but for the $^{12}\text{C} + ^{24}\text{Mg}$ reaction. Using sharp cut-off model in calculating the excitation function of this reaction and with $R_F = 7.8$ fm. The experimental data are taken from Ref. (14).

for fusion excitation functions with the experimental data [15] over the whole energy range is not possible except if we used the critical distance method which means that one should take another fusion at high energies which is smaller than the one used at low energies by

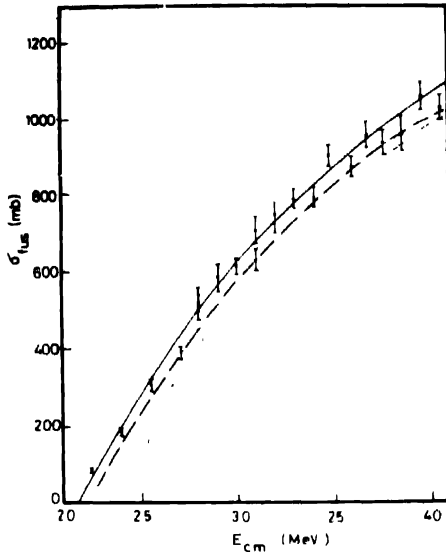


Figure 3. The same as Figure 2 but for the $^{24}\text{Mg} + ^{24}\text{Mg}$ reaction and with $R_F = 8.5$ fm. The experimental data are taken from Ref. (14).

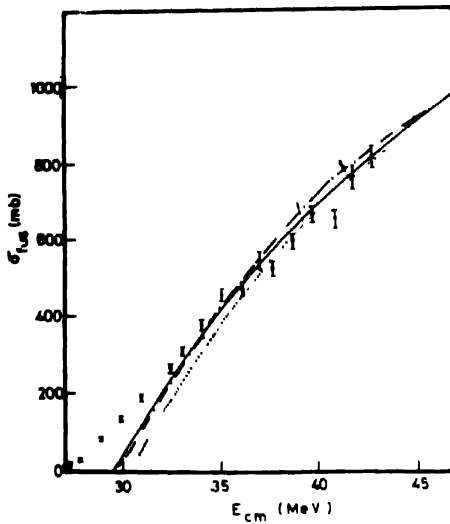


Figure 4. The same as Figure 2 but for the $^{28}\text{Si} + ^{30}\text{Si}$ reaction and with $R_F = 9.145$ fm. The experimental data are taken from Ref. (14).

using eqs. (9) and (10). This is known as Glas-Mosel model. Figure 9 presents the $^{16}\text{O} + ^{28}\text{Si}$ fusion cross section. The fusion radius $R_F = 8.6$ fm is adequate to fit the experimental data for fusion cross section at energies from $E_{c,m} = 20$ MeV to $E_{c,m} = 35$ MeV for

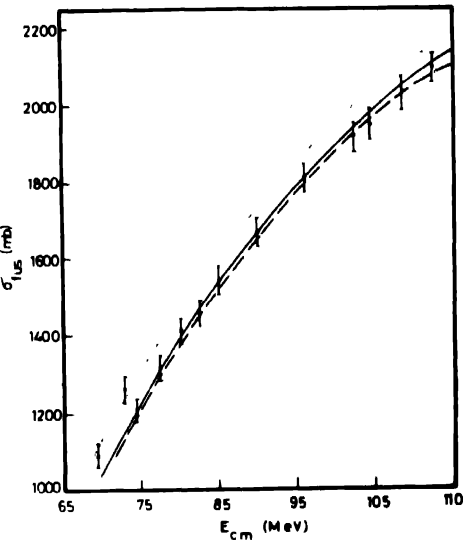


Figure 5. The same as Figure 2 but for the $^{175}\text{Lu} + ^{12}\text{C}$ reaction and with $R_F = 11.086$ fm. The experimental data are taken from Ref. (13).

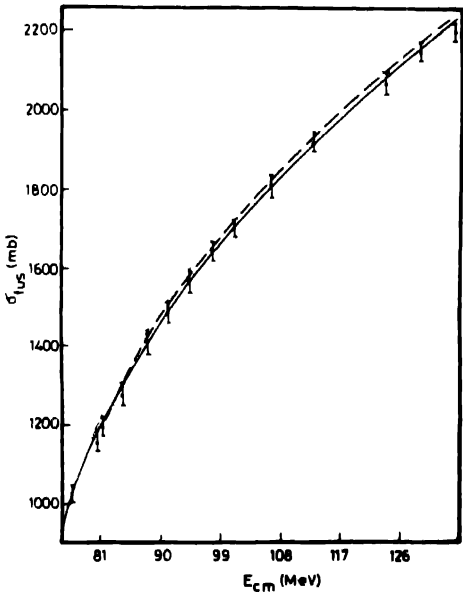


Figure 6. The same as Figure 2 but for the $^{165}\text{Ho} + ^{14}\text{N}$ reaction and with $R_F = 11.02$ fm. The experimental data are taken from Ref. (13).

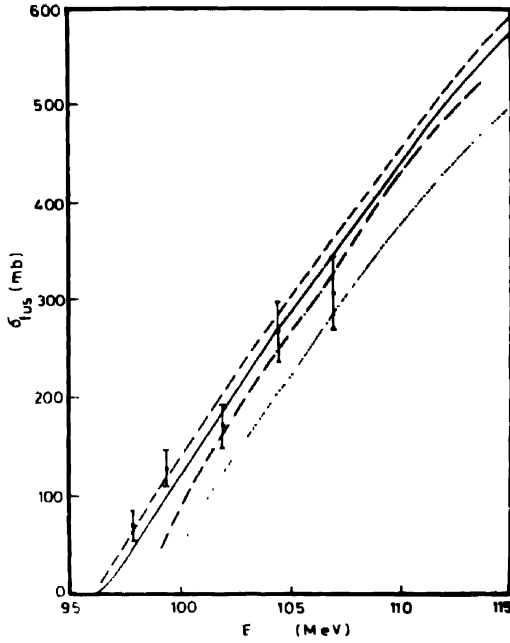


Figure 7. The calculated fusion cross section for the $^{64}\text{Ni} + ^{64}\text{Ni}$ reaction. (Dashed line) represents the calculation with sharp cut-off model and FDDM3Y force and with $R_F = 10.73$ fm. (Full line) represents the same calculation as dashed line but with smooth cut-off model and (dot-dashed) line is as that drawn in Figure 2

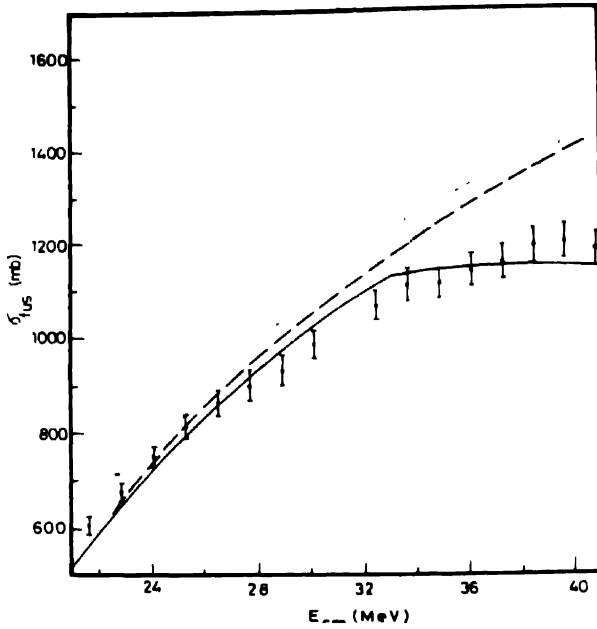


Figure 8. The same as in Figure 7 but for $^{16}\text{O} + ^{27}\text{Al}$ reaction and with $R_F = 8.746$ fm for energies smaller than 33 MeV. For energies greater than 33 MeV one takes another radius $R_{C_2} = 5.4$ fm to fit the experimental data which are taken from Ref. (15).

FDDM3Y and the other two common potentials while at energies greater than $E_{c,m} = 35$ MeV, the fusion radius which produce a good fit with the experimental data is $R_{Cr} = 5.17$.

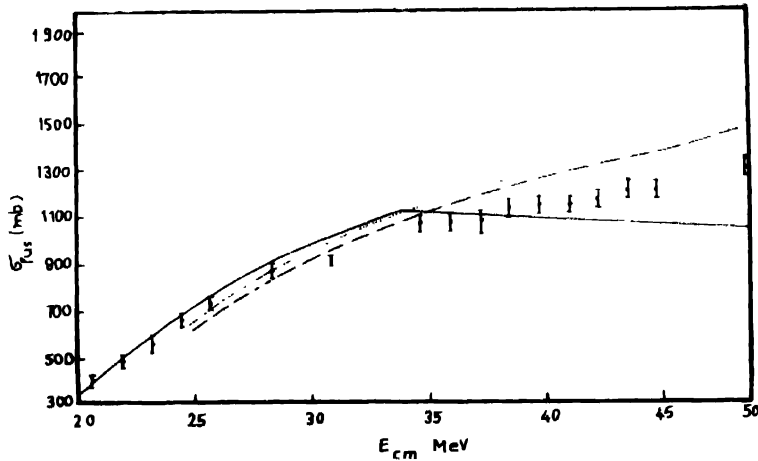


Figure 9. The same as in Figure 8 but for $^{16}\text{O} + ^{28}\text{Si}$ reaction and with $R_F = 8.6$ fm for energies smaller than 34 MeV. For energies greater than 34 MeV one takes another radius $R_{Cr} = 5.17$ fm to fit the experimental data which are taken from Ref. (15).

Galin [16] have noticed that an introduction of the concept of the critical distance is necessary. They found that the interaction distances for the fusion at high energies appear to have much smaller values. Glas and Mosel interpreted such a concept critical distance by setting $P_l = 0$ for $l > l_{cr}$ where the critical angular momentum l_{cr} satisfy the relation

$$\left[\frac{\hbar^2 l_{cr} (l_{cr} + 1)}{2\mu R_{Cr}^2} \right] + V_c(R_{Cr}) + V_n(R_{Cr}) = E.$$

The introduction of this critical distance means that those partial waves which penetrate the barrier but do not reach the closer distance R_{Cr} will not contribute to fusion channel. In this way, the fusion cross section is reduced at high energy. Also Figure 8 presents the $^{16}\text{O} + ^{27}\text{Al}$ fusion cross section. The fusion radius $R_F = 8.747$ fm is suitable to give a good fit with the experimental data for the energy range from $E_{c,m} = 20$ to 33 MeV but at energies greater than or equal to 33 MeV the adequate fusion radius used is $R_{Cr} = 5.4$ fm which gives the best fit with the experimental data.

We conclude from this study on the fusion excitation function for different pairs of nuclei that FDDM3Y-force is suitable for describing the two nucleon interaction force over a wide range of mass number and energies in comparison with the other the Woods-Saxon and the proximity potentials. Also the smooth cut-off approximation is better in some cases than the sharp cut-off approximation as it modifies the fitting with the experimental data especially at high energies as shown in the full line of Figure 7. It was noticed that some of the experimental results can be reproduced especially at high energies if we take

another critical radius R_C , different from R_F at lower energies. Therefore, it is interesting to study the fusion processes using attractive potential pockets with such depth and strength so as to keep the incident nuclei together long enough to be fused. However, the real problem remains in figuring out the imaginary part of the potential.

References

- [1] M Osman, H M M Mansour, M Ismail and Y A Lotfy 1989 *Nucl. Sci. J.* **26**
- [2] J S Lilley, B R Fulton, M A Nagarajan, I J Thompson and B W Banes 1985 *Phys. Lett.* **B151** 81
- [3] M El-Azab Farid and G R Satchler 1985 *Nucl. Phys.* **A438** 525
- [4] a) A K Chaudhuri and Bibach Sirha 1986 *Nucl. Phys.* **A455** 169
b) A K Chaudhuri 1986 *Nucl. Phys.* **A449** 243 and Refs. therein
- [5] M J Brown, V Obercker, M Seiwert and W Greiner 1983 *Z. Phys.* **310A** 287
- [6] H Ngô and Ch Ngô 1980 *Nucl. Phys.* **A348** 140
- [7] D Glas and U Mosel 1974 *Phys. Rev.* **C10** 2620
- [8] D Glas and U Mosel 1975 *Nucl. Phys.* **A237** 429
- [9] R Bass 1977 *Phys. Rev. Lett.* **39** (5) 265
- [10] L C Vaz and J M Alexander 1981 *Phys. Rep.* **69** 373
- [11] J R Birkelund and J R Huizenga 1983 *Ann. Rev. Nucl. Part. Sci.* **33** 265
- [12] D G Kovar 1979 *Phys. Rev.* **C20** 1305
- [13] J R Leigh, D J Hinde, J O Newton, W Galster and S H Sie 1982 *Phys. Lett.* **48** 527,
T Sikkeland, J E Clarkson, N H Steiger-Shafir and V E Viola 1971 *Phys. Rev.* **C3** 329
- [14] S Gary and C Volant 1982 *Phys. Rev.* **C25** 1877
- [15] H Oeschler, H Freisleben, K D Hildenbrand, P Engelstein, J P Coffin, B Heusch and P Wagner 1980 *Phys. Rev.* **C22** 546
- [16] J Galin, B Gatty, D Guerreau, C Rousset, U C Schlotthauer-Voos and X-Tarrago 1974 *Phys. Rev.* **C9** 1126